

Article

Protective Effects of Methoxsalen Supplementation on Chronic Alcohol-induced Osteopenia and Steatosis in Rats

Ju Ri Ham ¹, Ra-Yeong Choi ¹, Hae-In Lee ^{2,*}  and Mi-Kyung Lee ^{1,*} 

¹ Department of Food and Nutrition, Sunchon National University, Suncheon 57922, Korea; punsu05@nate.com (J.R.H.); fkdud1304@naver.com (R.-Y.C.)

² Mokpo Marin Food-Industry Research Center, Mokpo 58621, Korea

* Correspondence: hoch2731@nate.com (H.-I.L.); leemk@scnu.ac.kr (M.-K.L.); Tel.: +82-61-276-1670 (H.-I.L.); +82-61-750-3656 (M.-K.L.); Fax: +82-61-276-1673 (H.-I.L.); +82-61-750-3650 (M.-K.L.)

Received: 24 January 2020; Accepted: 4 March 2020; Published: 5 March 2020



Abstract: Osteopenia or osteoporosis occurs frequently in alcoholics and patients with alcoholic fatty liver disease. Methoxsalen (MTS), 8-methoxypsoralen, improved osteoporosis in ovariectomized and diabetic mouse models; however, its effects on alcohol-induced osteopenia and steatosis have not been reported. This study examined the effects of MTS on alcohol-induced bone loss and steatosis. Rats in the alcohol groups were fed a Liber-DeCarli liquid diet containing 36% of its calories as alcohol. MTS was at 0.005% in their diet, while alendronate (positive control; 500 µg/kg BW/day) was administered orally for eight weeks. The pair-fed group received the same volume of isocaloric liquid diet containing dextrin-maltose instead of alcohol as the alcohol control group consumed the previous day. In the alcohol-fed rats, the MTS and alendronate increased the bone volume density, bone surface density and trabecular number, while the bone specific surface, trabecular separation and structure model index were decreased in the tibia. MTS down-regulated tibial tartrate-resistant acid phosphatase 5 (*TRAP*) expression compared to the alcohol control group. MTS or alendronate prevented chronic alcohol-induced hepatic lipid accumulation and the triglyceride level in the alcohol-fed rats by decreasing the lipogenic enzyme activities and increasing the fatty acid oxidation enzyme activities. MTS reduced significantly the serum levels of alcohol, TRAP and tumor necrosis factor- α compared to the alcohol control group. Overall, these results suggest that MTS is likely to be an alternative agent for alcoholic osteopenia and hepatosteatois.

Keywords: alcohol; alendronate; bone quality; hepatosteatois; methoxsalen; osteopenia

1. Introduction

Chronic alcohol consumption-related diseases, including fatty liver disease, hepatitis, fibrosis and cirrhosis, are the leading causes of death for alcoholics [1]. Many studies have demonstrated that chronic and heavy alcohol intake is associated with impaired balanced bone remodeling and an increased risk of bone fragility [2]. Although the influence of alcohol on bone loss is controversial, alcohol-induced bone loss may eventually result in osteopenia, which has been attributed not only to the inhibition of bone synthesis but also to increased bone resorption through direct and indirect pathways [2]. Osteoporosis or osteopenia is a common complication of chronic liver disease, which is associated with age, BMI and alcohol liver disease [3]. Previous studies reported that patients with alcoholic liver diseases are more likely to have osteoporosis or osteopenia than those with chronic viral hepatitis [3,4]. Bisphosphonates and vitamin D supplementation have been used to prevent bone destruction and bone toxicity related to alcohol abuse in mice [5]. Many studies have examined natural plants and their bioactive compounds for preventing bone loss in the laboratory and in clinics [6,7].

Methoxsalen (8-methoxypsoralen, MTS), a natural photoactive compound, is found in various plants, such as celery, parsley, celeriac and lemon [8–10]. MTS is affiliated chemically to furanocoumarin, which has been used in combination with UVA irradiation as a photochemotherapeutic agent [11]. MTS has also been reported to have a range of physiological effects, including antioxidant [12], antiproliferative [13] and antimicrobial [14] activities. Moreover, MTS has anticancer effects, which increase the level of cytotoxicity in human hepatoma cells [15] and human osteosarcoma cells [16]. Previous studies showed that MTS has anti-osteoporosis effects in ovariectomized and diabetic mice [17,18], but the effects of MTS on alcoholic liver diseases have not been reported. Therefore, this study examined the efficacy and underlying mechanism of MTS on chronic alcohol-induced osteopenia and steatosis in rats.

2. Results

2.1. Bone Histomorphometric Parameters

Chronic alcohol feeding caused a loss of body weights; however, both MTS and alenderonate (AD) did not affect the body weight and feed efficiency ratio (data not shown).

Two-dimensional images of the distal femur and tibia showed that eight-week alcohol (36% of total energy) feeding induced bone-loss (Figure 1A,B), but MTS and AD reversed it, which was more effective on the tibia than the femur (Figure 1). For the alcohol control (Al-Con) group, the tibial bone volume density (BV/TV), bone surface density (BS/TV) and trabecular number (Tb.N) were significantly lower than that in the pair-fed (PF) group, whereas trabecular separation (Tb.Sp) and structure model index (SMI) were significantly higher (Figure 1C). For the MTS and AD groups, the tibial BV/TV, BS/TV and Tb.N were significantly higher than the Al-Con group and Tb.Sp and SMI were significantly lower (Figure 1C). No significant difference in bone mineral density (BMD) was observed between the two groups (Figure 1). Although the femoral microarchitectures did not show significant changes by alcohol, AD increased BV/TV, BS/TV and Tb.N, while decreased Tb.Sp and SMI compared to the Al-Con group (Figure 1D).

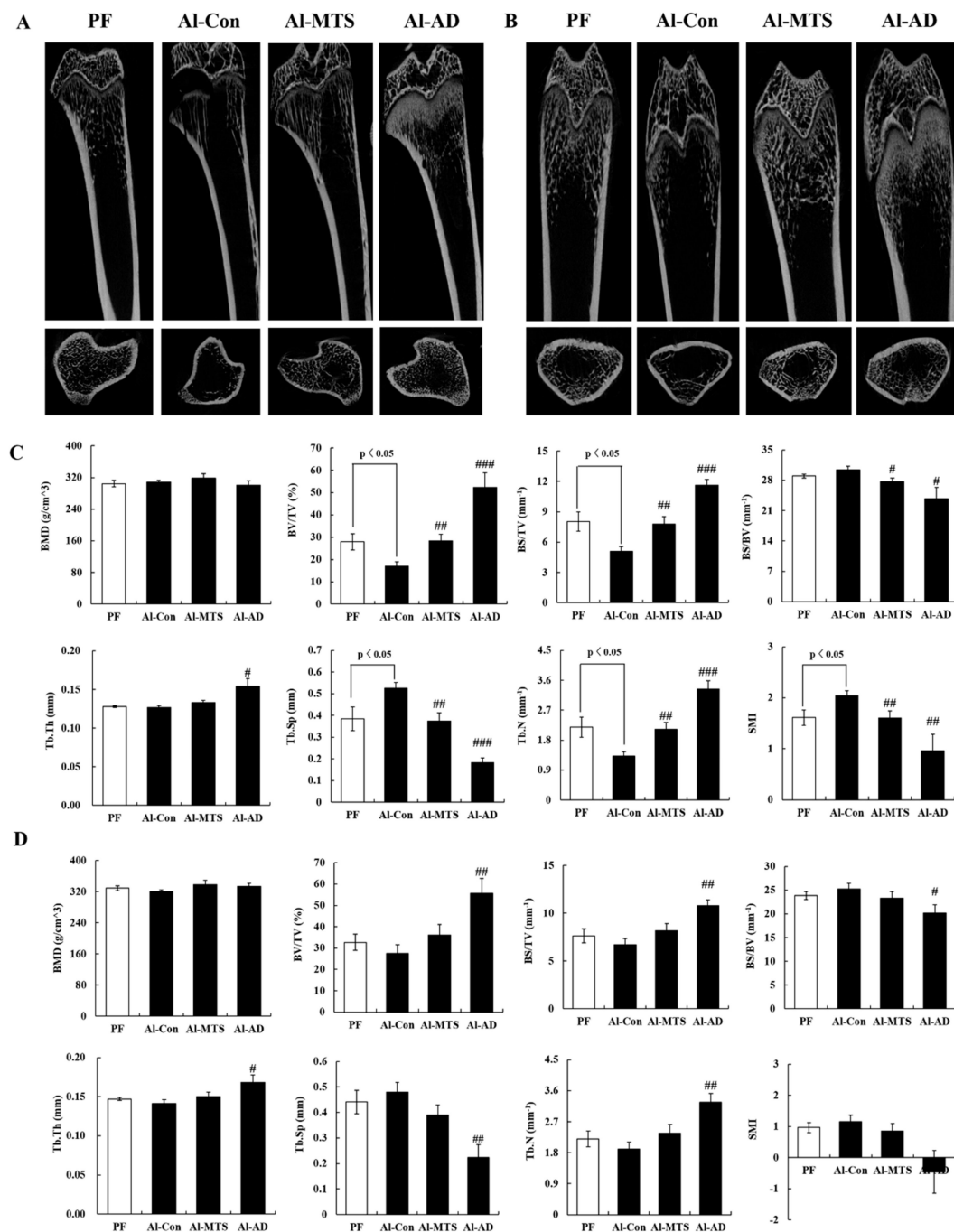


Figure 1. Effect of methoxsalen supplementation on the tibia micro-CT image (A), femur micro-CT image (B), tibia microarchitecture parameters (C) and femur microarchitecture parameters (D) in chronic alcohol-fed rats. The values are expressed as the mean \pm S.E. # $p < 0.05$, ## $p < 0.01$ and ### $p < 0.001$ vs. Al-Con according to a Student's *t*-test. PF; pair-fed, Al-Con: alcohol control, Al-MTS: alcohol supplemented with methoxsalen and Al-AD: alendronate.

2.2. Serum Bone Turnover Markers and Bone Remodeling-Related Gene Expression

The levels of bone formation marker, serum osteocalcin (OCN), were lower in the Al-Con group than in the PF group, but the decrease was not significant. The osteoclast differentiation-related factor, serum tartrate-resistant acid phosphatase 5 (TRAP) level, was significantly higher in the Al-Con group than in the PF group; however, MTS reduced the TRAP level significantly by 54.6%. AD did not alter

serum the TRAP level (Figure 2A). The serum calcium (Ca) level was lower in the Al-Con group than in the PF group. MTS and AD did not affect the serum Ca and inorganic phosphorus (IP) levels (Table 1).

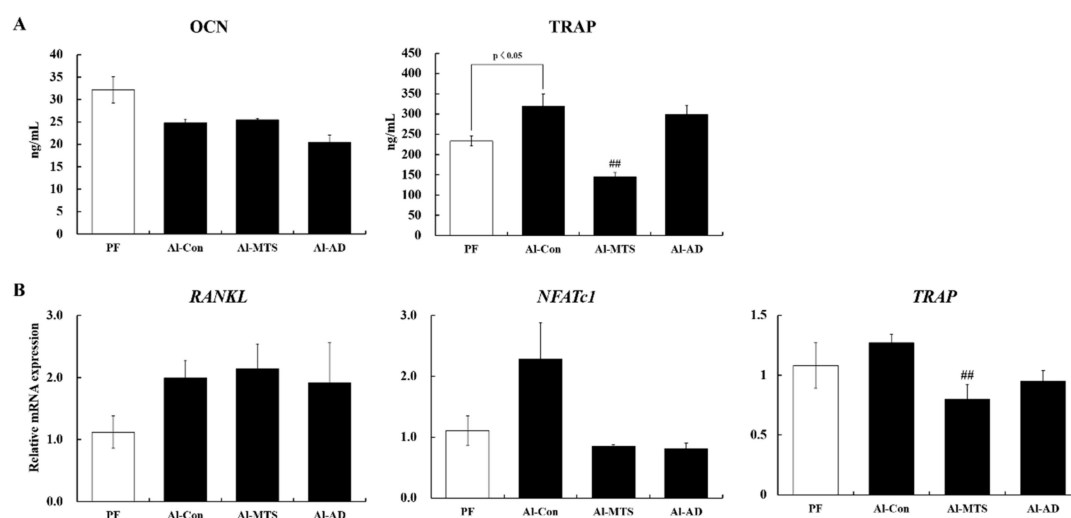


Figure 2. Effect of methoxsalen supplementation on serum osteocalcin (OCN) and tibial tartrate-resistant acid phosphatase 5 (TRAP) (A) and tibia osteoclast-related gene expression (B) in chronic alcohol-fed rats. The values are expressed as the mean \pm S.E. ## $p < 0.01$ vs. Al-Con according to a Student's t -test. RANKL: receptor activator of nuclear factor kappa-B ligand and NFATc1: nuclear factor of activated T-cells, cytoplasmic 1.

Table 1. Effects of methoxsalen supplementation on serum parameters in chronic alcohol-fed rats.

	PF	Al-Con	Al-MTS	Al-AD
Ca (U/L)	10.01 \pm 0.25	9.35 \pm 0.14 *	9.71 \pm 0.17	9.35 \pm 0.24
IP (U/L)	8.14 \pm 0.26	8.17 \pm 0.26	7.80 \pm 0.35	7.12 \pm 0.45
Alcohol (mg/L)	33.75 \pm 7.18	55.40 \pm 5.09 *	30.27 \pm 3.66 ##	28.12 \pm 5.92 ##
Acetaldehyde (mg/L)	41.85 \pm 11.62	66.57 \pm 19.37	28.22 \pm 5.03	22.90 \pm 3.45
AST (U/L)	94.20 \pm 9.34	374.80 \pm 93.30 *	194.80 \pm 24.63	319.83 \pm 68.09
ALT (U/L)	30.00 \pm 5.06	274.80 \pm 87.44 *	86.60 \pm 15.14	116.40 \pm 18.14
TNF- α (pg/mL)	208.67 \pm 23.43	299.62 \pm 19.86 *	131.45 \pm 34.99 ##	237.33 \pm 9.74 #
IL-6 (pg/mL)	4.33 \pm 0.16	3.92 \pm 0.17	3.56 \pm 0.21	3.40 \pm 0.09

Mean \pm SE. * $p < 0.05$ vs. pair-fed (PF), # $p < 0.05$ and ## $p < 0.01$ vs. alcohol control (Al-Con) according to a Student's t -test. Al-MTS: alcohol supplemented with methoxsalen, Al-AD: alenderonate, Ca: calcium, IP: inorganic phosphorus, AST: aspartate aminotransferase, ALT: alanine aminotransferase, TNF- α : tumor necrosis factor- α and IL-6: interleukin-6.

An upregulation trend in the gene expression of receptor activator of nuclear factor kappa-B ligand (RANKL) and nuclear factor of activated T-cells, cytoplasmic 1 (NFATc1), by 1.7- and 2.1-folds, respectively, was observed in the tibia of the Al-Con group compared to the PF group. On the other hand, MTS and AD normalized the value of NFATc1 expression (Figure 2B). In addition, MTS significantly down-regulated TRAP gene expression in the tibia compared to the Al-Con group (Figure 2B).

2.3. Hepatic Histology, Steatosis and Serum Alcohol Levels

As in Figure 3, hematoxylin and eosin (H&E) and Masson's Trichrome staining showed that chronic alcohol intake caused the enlargement of hepatocytes, an increase in the number of lipid droplets and fibrosis. However, MTS and AD normalized the number and size of the lipid droplets, as well as the formation of collagen (Figure 3). Compared to the Al-Con group, MTS decreased significantly the hepatic triglyceride (TG) content (33.0%) increased by alcohol (Table 2).

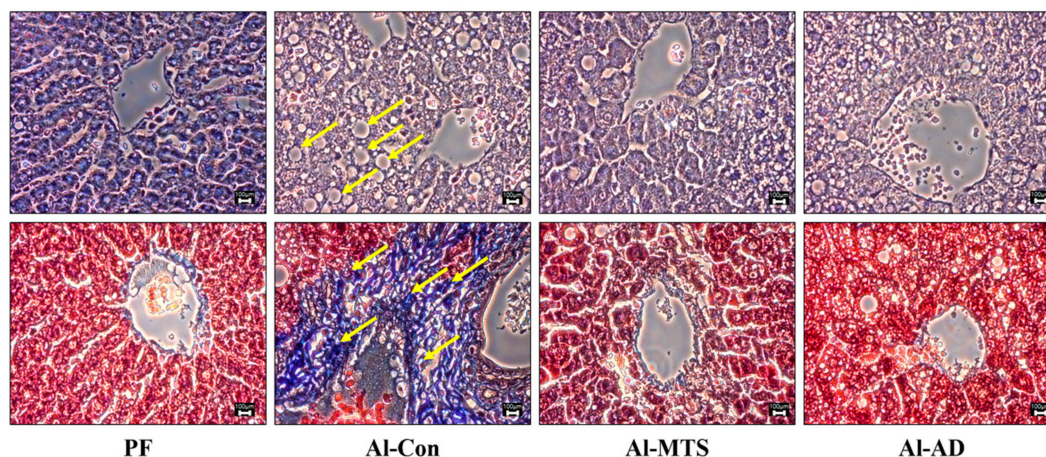


Figure 3. Effect of methoxsalen supplementation on hepatic hematoxylin and eosin and Masson's Trichrome staining in chronic alcohol-fed rats. Magnification 400×; the yellow arrows indicate lipid droplets and inflammation.

Table 2. Effects of methoxsalen supplementation on hepatic lipid contents and metabolic enzyme activities in chronic alcohol-fed rats.

	PF	AI-Con	AI-MTS	AI-AD
Hepatic lipid				
TG (mg/g)	20.33 ± 1.33	30.01 ± 41.75 **	20.11 ± 0.84 ##	29.94 ± 0.94
Cholesterol (mg/g)	3.90 ± 0.15	5.29 ± 0.23 **	4.78 ± 0.44	4.96 ± 0.50
FFA (mmol/g)	9.30 ± 0.92	11.61 ± 0.70	10.25 ± 0.49	11.40 ± 0.63
Enzyme activity				
ADH ¹⁾	384.77 ± 21.99	340.93 ± 8.61	347.45 ± 8.07	302.24 ± 15.16 #
ALDH ¹⁾	661.77 ± 24.08	671.40 ± 25.19	634.03 ± 43.12	620.51 ± 30.78
CYP2E1 ²⁾	17.99 ± 0.53	22.04 ± 1.35 *	16.65 ± 1.03 #	24.47 ± 1.35
FAS ³⁾	4.11 ± 0.15	4.36 ± 0.08	2.72 ± 0.21 ###	3.23 ± 0.35
PAP ²⁾	41.26 ± 3.45	69.48 ± 5.61 **	45.34 ± 4.15 #	71.94 ± 16.92
β-oxidation ²⁾	1.33 ± 0.13	1.19 ± 0.10	1.57 ± 0.12 #	1.55 ± 0.11 #
CPT ²⁾	11.32 ± 0.82	10.87 ± 0.33	12.54 ± 0.51 #	11.79 ± 0.81

Mean ± SE. * $p < 0.05$ and ** $p < 0.01$ vs. PF, # $p < 0.05$, ## $p < 0.01$ and ### $p < 0.001$ vs. AI-Con according to a Student's *t*-test. ¹⁾ pmol/min/mg protein, ²⁾ μmol/min/mg protein and ³⁾ nmol/min/mg protein. TG: triglyceride, FFA: free fatty acid, ADH: alcohol dehydrogenase, ALDH: aldehyde dehydrogenase 2, CYP2E1: cytochrome P450 2E1, FAS: fatty acid synthase, PAP: phosphatidate phosphohydrolase, CPT: carnitine palmitoyltransferase.

The serum alcohol level was significantly higher in the AI-Con group than in the PF group but MTS and AD lowered it (Table 1). MTS and AD also tended to lower the serum acetaldehyde level by 57.6% and 65.6%, respectively, compared to the AI-Con group (Table 1).

2.4. Serum Hepatotoxicity and Inflammatory Markers

MTS and AD decreased the aspartate aminotransferase (AST; 48.0% and 14.7%, respectively) and alanine aminotransferase (ALT; 68.5% and 57.6%, respectively) levels compared to the AI-Con group, but the decrease was not significant (Table 1). The serum cytokines, such as tumor necrosis factor-α (TNF-α) and interleukin-6 (IL-6), were measured to identify the effects of MTS on the inflammatory response. The TNF-α level was increased significantly in the AI-Con group, but MTS and AD decreased it by 56.1% and 20.8%, respectively. The IL-6 levels were similar in all groups (Table 1).

2.5. Hepatic Alcohol and Lipid Metabolic Enzyme Activities

Alcohol and MTS did not affect the hepatic alcohol dehydrogenase (ADH) and aldehyde dehydrogenase 2 (ALDH) activities, whereas AD decreased the ADH activity compared to the

Al-Con group (Table 2). The cytochrome P450 2E1 (CYP2E1) activity in the Al-Con group was significantly higher relative to the PF group; however, MTS recovered to near the value of PF (Table 2).

The phosphatidate phosphohydrolase (PAP) activity in the Al-Con group was higher than that in the PF group. However, MTS suppressed the lipid synthetic enzyme activities, such as fatty acid synthase (FAS) and PAP, 37.6% and 34.7%, respectively) compared to the Al-Con group, while it increased the carnitine palmitoyltransferase (CPT) and fatty acid β -oxidation (β -oxidation) activity. AD only increased the β -oxidation activity (Table 2).

3. Discussion

The effects of alcohol intake on bone health are controversial, but many studies have reported that chronic alcohol consumption affects bone remodeling, resulting in bone loss and an increased risk of osteoporosis and fractures [19,20]. The present study also found that chronic alcohol feeding during eight weeks reduced the trabecular bone mass and impaired the bone microarchitecture, leading to osteopenia. The bone BMD is a major marker of quantity, while bone quality is defined as the bone material properties, such as cortical and trabecular microarchitecture, mineralization, turnover and collagen content and structure [21]. Herein, the serum alcohol concentration was not associated with the BMD, but it was negatively related to BV/TV, trabecular thickness (Tb.Th.) and Tb.N. and positively related to Tb.Sp and SMI (data not shown), indicating that rats chronically fed 36% of their dietary calories as alcohol showed a reduced trabecular number, bone volume and thickness. On the other hand, MTS supplementation (0.005% in diet) effectively recovered the alcohol-induced osteopenia and detrimental effects on the bone microarchitecture, which was similar to that of AD (bisphosphonate drug against osteoporosis). AD is an aminobisphosphonate that inhibits bone resorption in osteoporotic human and rats [22]. In particular, the SMI is used to evaluate the characteristics of the rod and plate structure [23]. SMI in the Al-Con group was higher than PF, indicating that alcohol caused the formation of more rod structures, making them prone to fracture. However, both MTS and AD prevented the change in alcohol-induced rod-like structures in the tibia. Therefore, MTS prevented alcoholic osteopenia, as evidenced by the increased bone mass and bone quality.

The bone turnover markers have become an essential clinical tool for evaluating the bone structure [23]. In this study, MTS did not affect the serum OCN level (bone formation marker) but significantly lowered the serum TRAP (bone resorption marker) compared to the Al-Con group. TRAP is expressed in mature osteoclasts and plays a role in bone mineralization and skeletal development, indicating the amount and activity of osteoclast [24]. An increased TRAP level in the serum is associated with osteoporosis and other bone metabolic disorders [25]. Therefore, this study examined whether the protective effect of MTS against chronic alcohol-induced bone destruction is related to the changes in osteoclastogenesis-related genes. RANKL is an integral factor for osteoclast formation [26] and directly induced *NFATc1* expression, which stimulated RANKL-induced osteoclast differentiation [26]. Herein, *RANKL* and *NFATc1* expression had no statistical differences between Al-Con and PF, but alcohol led to a 1.7- and 2.1-fold increase in their expression, respectively, compared to PF. Iitsuka et al. [27] suggested that alcohol promoted osteoclastogenesis by increasing *RANKL* expression. *NFATc1* activates its target gene expression, such as *TRAP*, an osteoclast-specific sub-factor [28]. The present results showed that both MTS and AD similarly tend to down-regulate *NFATc1* and *TRAP* expression. In particular, MTS significantly suppressed *TRAP* expression, which led to a decrease in the serum TRAP level in chronic alcohol-fed rats. Therefore, the MTS-mediated decrease in TRAP is likely to be a key factor for improving the alcohol-induced osteopenia.

Alcoholic liver disease stimulates the release of cytokines, such as TNF- α , interleukin-1 β (IL-1 β) and IL-6, which promote the production RANKL and osteoclastogenesis [29]. A previous study showed that TNF- α is effectively accelerating RANKL production in osteoblasts, which increases osteoclasts formation [30]. This study found that chronic alcohol intake increases the serum TNF- α level compared to the PF group, but both MTS and AD effectively reversed these changes. Excessive alcohol consumption elevates the TNF- α level, which results in alcohol-related liver diseases, such as

fatty liver, hepatitis, cirrhosis and cancer [31]. Fatty liver disease (steatosis) is a condition where there is more than 5% fat deposition in hepatocytes. Chronic alcohol consumption leads to an increase in the supply of lipids from the small intestine to the liver [32], mobilization of fatty acids from the adipose tissue [33] and cholesterol synthesis [34] and decreases fatty acid oxidation in the liver [35]. The present study showed that chronic alcohol consumption causes hepatic steatosis, as evidenced by the accumulation of hepatic TG and morphological changes (lipid droplets and fibrosis of hepatocytes), as well as an elevation of the serums AST and ALT. Therefore, this study examined the role of MTS on alcoholic steatosis by determining the alcohol and lipid metabolism in the liver.

Alcohol is first metabolized to acetaldehyde and then to acetate [36]. Acetate converts to acetyl CoA, which can be used for energy or stored as a fat in the liver [37]. Excessive acetate leads to the accumulation of β -nicotinamide adenine dinucleotide and reduced disodium salt hydrate (NADH), which increases the level of fatty acid synthesis and TG deposition within the liver [38]. CYP2E1 can induce catalytic activity toward alcohol and generate a large amount of reactive oxygen species, which leads to alcoholic liver disease [38]. Therefore, reducing or suppressing CYP2E1 activity may be a practicable strategy for decreasing the hepatotoxicity of alcohol [39]. Lu et al. [40] examined whether CYP2E1 contributes to alcoholic fatty liver disease using CYP2E1-knockout mice and suggested that CYP2E1-derived oxidative stress inhibits fatty acid oxidation, resulting in fatty liver disease. Our results also showed that the alcohol induced hepatic CYP2E1 activity and the accumulation of lipids, but MTS lowered the hepatic TG levels and lipid droplets significantly compared to the AI-Con group. A previous study reported that increased hepatic PAP activity was involved in the TG deposit in chronic alcohol-fed rats [41]. A similar change was observed in the present study. MTS significantly suppressed the FAS and PAP activities, which were increased by chronic alcohol intake. PAP and FAS are major enzymes in the TG and fatty acid synthesis pathways in the liver. On the other hand, hepatic CPT is a major enzyme of the fatty acid oxidation pathway. The inhibition of CPT leads to a decrease in fatty acid oxidation and a further increase in hepatic TG accumulation [42]. In this study, MTS elevated the level of fatty acid oxidation significantly in the liver of chronically alcohol-fed rats by stimulating CPT and β -oxidation. Interestingly, the hepatic TG concentration was positively correlated with the PAP activities and negatively correlated with CPT (data not shown). Therefore, MTS suppressed the lipogenesis (FAS and PAP) activities and increased the fatty acid oxidation (CPT and β -oxidation) activity, which may have helped to improve hepatic steatosis.

4. Materials and Methods

4.1. Animals and Experimental Design

Sprague-Dawley rats (eight-week-old males) were purchased from Orient Bio Inc. (Seongnam, Korea) and housed individually under a 12-h light/12-h dark illumination cycle, 50% \pm 5% humidity, and 20 \pm 2 °C. The animals were used in accordance with the institutional guidelines, and the procedures were approved by the Institutional Animal Care and Use Committee of Suncheon National University (approval No. SCNU_IACUC-2018-03).

The animals were acclimatized for one week (chow and water ad libitum) and then divided randomly into the following four groups:

Group 1: pair-fed group (PF),

Group 2: alcohol control group (AI-Con),

Group 3: 0.005 % MTS (in diet) was supplemented with alcohol (AI-MTS) and

Group 4: alendronate (500 μ g/kg BW/day, oral) was administered alcohol (AI-AD).

The alcohol-fed groups were introduced to an alcohol-containing liquid diet with a step-wise increase in alcohol: days 1 and 2, 3% alcohol (21% of the total energy); days 3 and 4, 4% alcohol (28% of the total energy) and after day 5, 5% alcohol (36% of the total energy). Group 1 was pair-fed and received the same volume of isocaloric liquid diet containing dextrin-maltose instead of alcohol as Group 2 consumed the previous day.

After eight weeks, the rats were anesthetized with CO₂ gas after 12 h of food deprivation. Blood samples were then taken from the inferior vena cava. The serum was obtained by centrifuging the blood at 3000 rpm for 15 min at 4 °C. The organs (liver and bone tissues) were then removed, rinsed with physiological saline and weighed immediately.

4.2. Biomarkers In Serum

The alcohol and acetaldehyde levels were determined using an enzymatic bioassay (Megazyme, Chicago, IL, USA). The OCN, TRAP, TNF- α and IL-6 levels were determined using a quantitative sandwich enzyme immunoassay (ELISA) kit (Elabscience Biotechnology Co., Ltd, Wuhan, China). AST, ALT, Ca and IP levels were measured using a diagnostic slide kit and an automatic analyzer (Dri-chem 3500i; Fujifilm Medical System Co., Ltd, Tokyo, Japan).

4.3. Micro-Computed Tomography (Micro-CT) Assay

After cleaning the adherent soft bone tissues and storing the bones in 70% ethyl alcohol, the femurs and tibias were analyzed using a high-resolution Skyscan micro-CT system (Skyscan 1272; Bruker, Billerica, MA, USA) and software as described previously [18]. The samples were scanned using a voxel size of 20.6 μ m at 70 kV and 142 μ A. Two-dimensional images were obtained for visualization and display. For morphometric analysis, the following structural parameters were calculated as a region of interest (ROI) of cancellous bone using CTAn (Bruker, Billerica, MA, USA). The BMD, BV/TV, BS/TV, bone specific surface (BS/BV), Tb.Th, Tb.Sp, Tb.N and SMI of each samples were then calculated.

4.4. Quantitative Real-Time PCR Analysis in Bone

The tibia was homogenized in TriZol reagent (Invitrogen, Carlsbad, CA, USA); after which, the total RNA was isolated according to the manufacturer's specifications. The total RNA (1 μ g) was then reverse-transcribed into cDNA using a ReverTra Ace qPCR RT master mix (Toyobo, Osaka, Japan). The level of mRNA expression was then quantified by real-time quantitative PCR using a SYBR green PCR kit (Qiagen, Hilden, Germany) and a CFX96TM real-time system (Bio-Rad, Hercules, CA, USA). The primer sequences are shown in the Supplementary File. The cycle thresholds were determined based on the SYBR green emission intensity during the exponential phase, and the fold changes were determined using the $2^{-\Delta\Delta C_t}$ method [43]. In addition, transcripts of β -actin (*Actb*) were amplified from the samples to ensure normalized real-time quantitative RT-PCR detection.

4.5. Histological and Lipid Contents Analysis in Liver

For histological analysis, the liver was fixed in a buffer solution containing 10% formalin, processed routinely and embedded in paraffin. Blocks were cut to a 3–5- μ m thickness, and sections were cut on glass slides and stained with H&E and Masson's Trichrome. The stained area was then viewed using an optical microscope at 400 \times magnification.

The hepatic lipids were extracted, as described previously [44]; after which, the TG, cholesterol (Asan Pharmaceutical Co., Ltd., Seoul, Korea) and free fatty acid (FFA) (Shinyang Diagnostics, Seoul, Korea) concentrations were determined using commercial kits.

4.6. Enzyme Activities in Liver

The following were determined as described previously: alcohol metabolic enzymes such as ADH, ALDH and CYP2E1 activities [41]; lipid metabolic enzymes activities such as FAS and PAP and β -oxidation and CPT activities [45].

4.7. Statistical Analysis

All data are presented as the means \pm standard error (SE). Statistical analyses were conducted using the SPSS statistical software version 25.0 (SPSS Inc., Chicago, IL, USA). Comparisons between the groups were evaluated using a Student's *t*-test. A *p*-value < 0.05 was considered significant.

5. Conclusions

These findings are the first to show that MTS alleviates the chronic alcohol-induced deleterious changes in bone quality and steatosis through the modification of osteoclastogenesis and lipid metabolism. These features make MTS a promising candidate for the prevention of alcohol-induced bone loss and steatosis.

Supplementary Materials: The following are available online.

Author Contributions: Conceptualization, J.R.H., R.-Y.C., H.-I.L. and M.-K.L.; data curation, J.R.H.; formal analysis, J.R.H., R.-Y.C. and M.-K.L.; investigation, J.R.H. and R.-Y.C.; methodology, J.R.H.; supervision, M.-K.L.; writing—original draft, J.R.H. and M.-K.L. and writing—review and editing, H.-I.L. and M.-K.L. All authors have read and agreed to the published version of the manuscript.

Funding: This work was supported by Basic Science Research Program through the National Research Foundation of Korea (NRF) funded by the Ministry of Education (No. NRF-2015R1C1A2A01052146).

Conflicts of Interest: The authors declare no conflict of interest.

References

1. Rong, S.; Zhao, Y.; Bao, W.; Xiao, X.; Wang, D.; Nussler, A.K.; Yan, H.; Yao, P.; Liu, L. Curcumin prevents chronic alcohol-induced liver disease involving decreasing ROS generation and enhancing antioxidative capacity. *Phytomedicine* **2012**, *19*, 545–550. [[CrossRef](#)] [[PubMed](#)]
2. Luo, Z.; Liu, Y.; Liu, Y.; Chen, H.; Shi, S.; Liu, Y. Cellular and molecular mechanisms of alcohol-induced osteopenia. *Cell. Mol. Life Sci.* **2017**, *74*, 4443–4453. [[CrossRef](#)] [[PubMed](#)]
3. Zheng, J.P.; Miao, H.X.; Zheng, S.W.; Liu, W.L.; Chen, C.Q.; Zhong, H.B.; Li, S.F.; Fang, Y.P.; Sun, C.H. Risk factors for osteoporosis in liver cirrhosis patients measured by transient elastography. *Medicine (Baltimore)* **2018**, *97*, e10645. [[CrossRef](#)] [[PubMed](#)]
4. González-Reimers, E.; García-Valdecasas-Campelo, E.; Santolaria-Fernández, F.; Milena-Abril, A.; Rodríguez-Rodríguez, E.; Martínez-Riera, A.; Pérez-Ramírez, A.; Alemán-Vallas, M.R. Rib fractures in chronic alcoholic men: Relationship with feeding habits, social problems, malnutrition, bone alterations, and liver dysfunction. *Alcohol* **2005**, *37*, 113–117. [[CrossRef](#)]
5. Mercer, K.E.; Wynne, R.A.; Lazarenko, O.P.; Lumpkin, C.K.; Hogue, W.R.; Suva, L.J.; Chen, J.R.; Mason, A.Z.; Badger, T.M.; Ronis, M.J. Vitamin D supplementation protects against bone loss associated with chronic alcohol administration in female mice. *J. Pharmacol. Exp. Ther.* **2012**, *343*, 401–412. [[CrossRef](#)] [[PubMed](#)]
6. An, J.; Yang, H.; Zhang, Q.; Liu, C.; Zhao, J.; Zhang, L.; Chen, B. Natural products for treatment of osteoporosis: The effects and mechanisms on promoting osteoblast-mediated bone formation. *Life Sci.* **2016**, *147*, 46–58. [[CrossRef](#)]
7. Leung, P.C.; Siu, W.S. Herbal treatment for osteoporosis: A current review. *J. Tradit. Complement. Med.* **2013**, *3*, 82–87. [[CrossRef](#)]
8. Chaudhary, S.K.; Ceska, O.; Warrington, P.J.; Ashwood-Smith, M.J. Increased furocoumarin content of celery during storage. *J. Agric. Food Chem.* **1985**, *33*, 1153–1157. [[CrossRef](#)]
9. Melough, M.M.; Lee, S.G.; Cho, E.; Kim, K.; Provatas, A.A.; Perkins, C.; Park, M.K.; Qureshi, A.; Chun, O.K. Identification and quantitation of furocoumarins in popularly consumed foods in the US Using QuEChERS extraction coupled with UPLC-MS/MS analysis. *J. Agric. Food Chem.* **2017**, *65*, 5049–5055. [[CrossRef](#)]
10. Radziejewska-Kubzdela, E.; Czapski, J.; Czaczyk, K.; Biegańska-Marecik, R. The effect of pre-treatment and modified atmosphere packaging on contents of phenolic compounds and sensory and microbiological quality of shredded celeriac. *J. Sci. Food Agric.* **2014**, *94*, 1140–1148. [[CrossRef](#)]

11. Engin, B.; Oguz, O. Evaluation of time-dependent response to psoralen plus UVA (PUVA) treatment with topical 8-methoxypsoralen (8-MOP) gel in palmoplantar dermatoses. *Int. J. Dermatol.* **2005**, *44*, 337–339. [[CrossRef](#)] [[PubMed](#)]
12. Senol, F.S.; Woźniak, K.S.; Khan, M.T.H.; Orhan, I.E.; Sener, B.; Głowniak, K. An in vitro and in silico approach to cholinesterase inhibitory and antioxidant effects of the methanol extract, furanocoumarin fraction, and major coumarins of *Angelica officinalis* L. fruits. *Phytochem. Lett.* **2011**, *4*, 462–467. [[CrossRef](#)]
13. Sumiyoshi, M.; Sakanaka, M.; Taniguchi, M.; Baba, K.; Kimura, Y. Anti-tumor effects of various furocoumarins isolated from the roots, seeds and fruits of *Angelica* and *Cnidium* species under ultraviolet A irradiation. *J. Nat. Med.* **2014**, *68*, 83–94. [[CrossRef](#)] [[PubMed](#)]
14. Walasek, M.; Grzegorzczak, A.; Malm, A.; Skalicka-Woźniak, K. Bioactivity-guided isolation of antimicrobial coumarins from *Heracleum mantegazzianum* Sommier & Levier (Apiaceae) fruits by high-performance counter-current chromatography. *Food Chem.* **2015**, *186*, 133–138. [[PubMed](#)]
15. Peng, Y.; Liu, W.; Xiong, J.; Gui, H.Y.; Feng, X.M.; Chen, R.N.; Hu, G.; Yang, J. Down regulation of differentiated embryonic chondrocytes 1 (DEC1) is involved in 8-methoxypsoralen-induced apoptosis in HepG2 cells. *Toxicology* **2012**, *301*, 58–65. [[CrossRef](#)] [[PubMed](#)]
16. Lu, T.C.; Chou, C.T.; Liang, W.Z.; Kuo, C.C.; Hsu, S.S.; Wang, J.L.; Jan, C.R. Effect of methoxsalen on Ca²⁺ homeostasis and viability in human osteosarcoma cells. *Chin. J. Physiol.* **2017**, *60*, 174–182. [[CrossRef](#)] [[PubMed](#)]
17. Ham, J.R.; Choi, R.Y.; Yee, S.T.; Hwang, Y.H.; Kim, M.J.; Lee, M.K. Methoxsalen supplementation attenuates bone loss and inflammatory response in ovariectomized mice. *Chem. Biol. Interact.* **2017**, *278*, 135–140. [[CrossRef](#)]
18. Ham, J.R.; Choi, R.Y.; Lee, H.I.; Lee, M.K. Methoxsalen and bergapten prevent diabetes-induced osteoporosis by the suppression of osteoclastogenic gene expression in mice. *Int. J. Mol. Sci.* **2019**, *20*, 1298. [[CrossRef](#)]
19. Maruel, D.B.; Boisseau, N.; Benhamou, C.L.; Jaffre, C. Alcohol and bone: review of dose effects and mechanisms. *Osteoporosis Int.* **2012**, *23*, 1–16. [[CrossRef](#)]
20. Turner, R.T. Skeletal response to alcohol. *Alcohol. Clin. Exp. Res.* **2000**, *24*, 1693–1701. [[CrossRef](#)]
21. McNerny, E.M.B.; Nickolas, T.L. Bone quality in chronic kidney disease: definitions and diagnostics. *Curr. Osteoporosis Rep.* **2017**, *15*, 207–213. [[CrossRef](#)] [[PubMed](#)]
22. Wezeman, F.H.; Emanuele, M.A.; Moskal, S.F.; Steiner, J.; Lapaglia, N. Alendronate administration and skeletal response during chronic alcohol intake in the adolescent male rat. *J. Bone Miner. Res.* **2000**, *15*, 2033–2041. [[CrossRef](#)] [[PubMed](#)]
23. Hildebrand, T.; Rügsegger, P. Quantification of bone microarchitecture with the structure model index. *Comput. Methods Biomech. Biomed. Eng.* **1997**, *1*, 15–23. [[CrossRef](#)] [[PubMed](#)]
24. Kang, I.S.; Kim, C. Taurine chloramine inhibits osteoclastic differentiation and osteoclast marker expression in RAW 264.7 cells. *Adv. Exp. Med. Biol.* **2019**, *1155*, 61–70. [[PubMed](#)]
25. Deyhim, F.; Garica, K.; Lopez, E.; Gonzalez, J.; Ino, S.; Garcia, M.; Patil, B.S. Citrus juice modulates bone strength in male senescent rat model of osteoporosis. *Nutrition* **2006**, *22*, 559–563. [[CrossRef](#)]
26. Wang, W.; Wu, C.; Tian, B.; Liu, X.; Zhai, Z.; Qu, X.; Jiang, C.; Ouyang, Z.; Mao, Y.; Tang, T.; et al. The inhibition of RANKL-induced osteoclastogenesis through the suppression of p38 signaling pathway by naringenin and attenuation of titanium-particle-induced osteolysis. *Int. J. Mol. Sci.* **2014**, *15*, 21913–21934. [[CrossRef](#)]
27. Iitsuka, N.; Hie, M.; Nakanishi, A.; Tsukamoto, I. Ethanol increases osteoclastogenesis associated with the increased expression of RANK, PU. 1 and MITF in vitro and in vivo. *Int. J. Mol. Med.* **2012**, *30*, 165–172.
28. Teitelbaum, S.L. Bone resorption by osteoclasts. *Science* **2000**, *289*, 1504–1508. [[CrossRef](#)]
29. Bu, R.; Borysenko, C.W.; Li, Y.; Cao, L.; Sabokbar, A.; Blair, H.C. Expression and function of TNF-family proteins and receptors in human osteoblasts. *Bone* **2003**, *33*, 760–770. [[CrossRef](#)]
30. Pietschmann, P.; Mechtcheriakova, D.; Meshcheryakova, A.; Föger-Samwald, U.; Ellinger, I. Immunology of osteoporosis: A mini-review. *Gerontology* **2016**, *62*, 128–137. [[CrossRef](#)]
31. Kawaratani, H.; Tsujimoto, T.; Douhara, A.; Takaya, H.; Moriya, K.; Namisaki, T.; Noguchi, R.; Yoshiji, H.; Fujimoto, M.; Fukui, H. The effect of inflammatory cytokines in alcoholic liver disease. *Mediators Inflamm.* **2013**, *2013*, 495156–495165. [[CrossRef](#)] [[PubMed](#)]
32. Hartmann, P.; Hochrath, K.; Horvath, A.; Chen, P.; Seebauer, C.T.; Llorente, C.; Wang, L.; Alnouti, Y.; Fouts, D.E.; Stärkel, P.; et al. Modulation of the intestinal bile acid/farnesoid X receptor/fibroblast growth factor 15 axis improves alcoholic liver disease in mice. *Hepatology* **2018**, *67*, 2150–2166. [[CrossRef](#)] [[PubMed](#)]

33. Harmon, D.B.; Wu, C.; Dedousis, N.; Sipula, I.J.; Stefanovic-Racic, M.; Schoiswohl, G.; O'Donnell, C.P.; Alonso, L.C.; Kershaw, E.E.; Kelley, E.E.; et al. Adipose tissue-derived free fatty acids initiate myeloid cell accumulation in mouse liver in states of lipid oversupply. *Am. J. Physiol. Endocrinol. Metab.* **2018**, *315*, E758CE770. [[CrossRef](#)] [[PubMed](#)]
34. Delgado-Villa, M.J.; Ojeda, M.L.; Rubio, J.M.; Murillo, M.L.; Sánchez, O.C. Beneficial role of dietary folic acid on cholesterol and bile acid metabolism in ethanol-fed rats. *J. Stud. Alcohol Drugs* **2000**, *70*, 615–622. [[CrossRef](#)] [[PubMed](#)]
35. Blomstrand, R.; Kager, L. The combustion of triolein-1-14C and its inhibition by alcohol in man. *Life Sci.* **1973**, *13*, 113–123. [[CrossRef](#)]
36. Cederbaum, A.I. Alcohol metabolism. *Clin. Liver Dis.* **2012**, *16*, 667–685. [[CrossRef](#)]
37. Gaddini, G.W.; Turner, R.T.; Grant, K.A.; Iwaniec, U.T. Alcohol: a simple nutrient with complex actions on bone in the adult skeleton. *Alcohol. Clin. Exp. Res.* **2016**, *40*, 657–671. [[CrossRef](#)]
38. Zima, T. Alcohol abuse. *EJIFCC.* **2018**, *29*, 285–289.
39. Kojima-Yuasa, A.; Goto, M.; Yoshikawa, E.; Morita, Y.; Sekiguchi, H.; Sutoh, K.; Usumi, K.; Matsui-Yuasa, I. Protective effects of hydrolyzed nucleoproteins from Salmon Milt against ethanol-induced liver injury in rats. *Mar. Drugs* **2016**, *14*, 232. [[CrossRef](#)]
40. Lu, Y.; Zhuge, J.; Wang, X.; Bai, J.; Cederbaum, A.I. Cytochrome P450 2E1 contributes to ethanol-induced fatty liver in mice. *Hepatology* **2008**, *47*, 1483–1494. [[CrossRef](#)]
41. Choi, R.Y.; Woo, M.J.; Ham, J.R.; Lee, M.K. Anti-steatotic and anti-inflammatory effects of *Hovenia dulcis* Thunb. extracts in chronic alcohol-fed rats. *Biomed. Pharmacother.* **2017**, *90*, 393–401. [[CrossRef](#)] [[PubMed](#)]
42. Serviddio, G.; Giudetti, A.M.; Bellanti, F.; Priore, P.; Rollo, T.; Tamborra, R.; Siculella, L.; Vendemiale, G.; Altomare, E.; Gnoni, G.V. Oxidation of hepatic carnitine palmitoyl transferase-I (CPT-I) impairs fatty acid beta-oxidation in rats fed a methionine-choline deficient diet. *PLoS ONE* **2011**, *6*, e24084. [[CrossRef](#)] [[PubMed](#)]
43. Livak, K.J.; Schmittgen, T.D. Analysis of relative gene expression data using real-time quantitative PCR and the $2^{-\Delta\Delta CT}$ method. *Methods* **2001**, *25*, 402–408. [[CrossRef](#)] [[PubMed](#)]
44. Lee, H.I.; Seo, K.O.; Yun, K.W.; Kim, M.J.; Lee, M.K. Comparative study of the hepatoprotective efficacy of *Artemisia iwayomogi* and *Artemisia capillaris* on ethanol-administered mice. *J. Food Sci.* **2011**, *76*, 207–211. [[CrossRef](#)]
45. Ham, J.R.; Lee, H.I.; Choi, R.Y.; Sim, M.O.; Seo, K.I.; Lee, M.K. Anti-steatotic and anti-inflammatory roles of syringic acid in high-fat diet-induced obese mice. *Food Funct.* **2016**, *7*, 689–697. [[CrossRef](#)]

Sample Availability: Samples of the compounds are not available from the authors.



© 2020 by the authors. Licensee MDPI, Basel, Switzerland. This article is an open access article distributed under the terms and conditions of the Creative Commons Attribution (CC BY) license (<http://creativecommons.org/licenses/by/4.0/>).